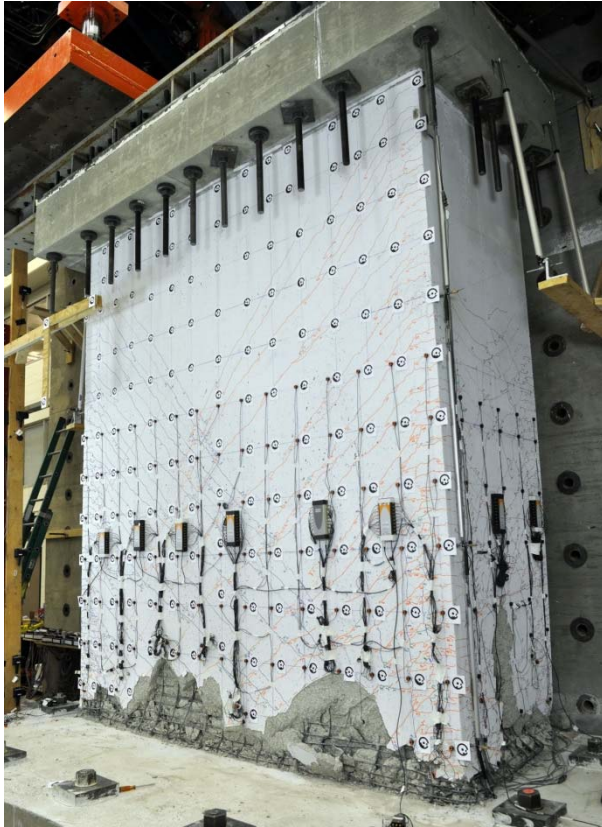


Recommendations for Seismic Demand and Performance Assessment for Flexural Concrete Walls



Dr. Laura Lowes, University of Washington
Dr. Dawn Lehman, University of Washington

Funding provided by the **National Science Foundation** and the **Charles Pankow Foundation**

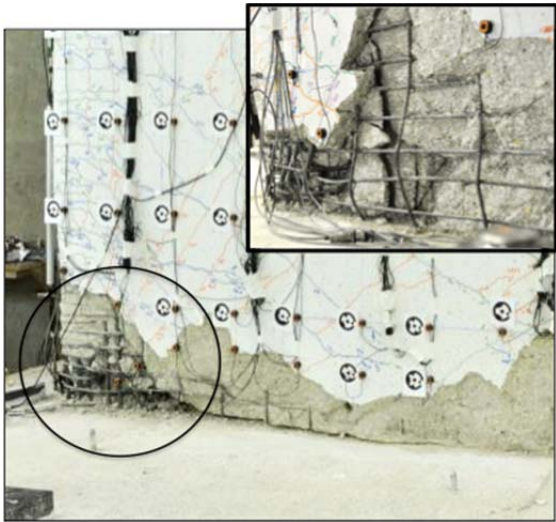


RECOMMENDATIONS FOR SEISMIC DEMAND AND PERFORMANCE ASSESSMENT FOR FLEXURAL CONCRETE WALLS

Laura N. Lowes and Dawn E. Lehman, University of Washington

INTRODUCTION

Structural concrete walls are one of the most common lateral load resisting systems as they provide high stiffness under service-level loading and high strength under design-level loading. However, recent earthquakes and experimental testing have demonstrated that walls and walled buildings are vulnerable to damage, including shear and compression failures (Table 1).

Table 1: Different Performance States of Wall Components and Wall Buildings Designed to Meet Different Code Requirements	
	
(a) Shear failure (Moehle 2012)	(b) Damage at multiple locations (Moehle 2012)
	
(c) Compression damage	(d) Collapse of walled building (Moehle 2012)

Research was conducted to improve understanding of the seismic behavior of flexural concrete walls and develop recommendations for advancing seismic design of walled buildings. Research activities included experimental testing, analysis of experimental data for walls tested by the

research team and others, development of nonlinear response models, and application of these models to assess walled building response under earthquake loading. Ultimately, these activities resulted in i) improved methods for using linear analysis to determine seismic demands for use in design of flexural walls, ii) improved nonlinear analysis methods for response assessment of flexural walls, and iii) performance-prediction models (i.e. fragility functions) for flexural walls in walled buildings.

Research results are summarized here, within the context of a proposed design procedure for concrete walled buildings. This design procedure is intended to result in walls that achieve a ductile tension-controlled flexural response mechanism, shear demands that do not exceed those used for design, flexural yielding isolated to locations identified by the engineer, and low collapse probabilities for design-basis and maximum-considered earthquake demand levels.

The proposed design process is as followings:

1. Provide the layout of walls throughout the building floor plan.
2. Determine wall cross-sectional configuration.
3. Estimate lateral forces for use in design of the system. Note that these forces are computed using a response modification factor (R), which may depend on the wall design and expected response.
4. Estimate wall thickness using estimated axial and shear demands and recommended stress limits.
5. Using initial estimates of wall layout, configuration, and size (thickness) conduct demand analysis. Typically the demand analysis will be an elastic modal analysis. This type of analysis uses elastic elements for the wall (either line elements or shell elements, depending on the type of software) and requires an effective stiffness for those elements.
6. Design flexural reinforcement.
7. Repeat demand analyses as required. In some cases nonlinear analyses are conducted to provide a more accurate estimate of the time-dependent and maximum deformations and demands resulting from ductile yielding of wall components. Nonlinear analyses are typically conducted for walled buildings with a height greater than 240 ft.
8. Size and detail wall horizontal reinforcement to meet shear demands resulting from a proposed capacity-design approach. If resizing of wall is required, steps 5-8 must be repeated.
9. Size and detail confining reinforcement to meet ACI Code requirements. Detailing to achieve ductile response was not directly investigated as part of this research effort, and guidance for detailing is not addressed in this document.
10. If appropriate, conduct performance assessment using linear or nonlinear analysis results. Probabilistic performance-prediction models (i.e. fragility functions) may be used here. Fragility functions often define the likelihood of damage given maximum story drift demand. While drift demand can be estimated using the results of linear analysis, the use of nonlinear analysis results is recommended to improve accuracy.

The following sections present information to guide the engineer in conducting this process.

WALL CONFIGURATION

Walls are typically configured to meet architectural constraints. Figure 1 shows commonly used configurations. In low-rise buildings, there is not typically a single large core, and walls are placed near openings, including stairs, mechanical shafts, and elevator cores. In mid- to high-rise construction, core walls are typically used to form openings for elevator shafts (see the core wall configuration at the bottom of Figure 1). As a result, asymmetric wall configurations are more common in low-rise walled buildings.

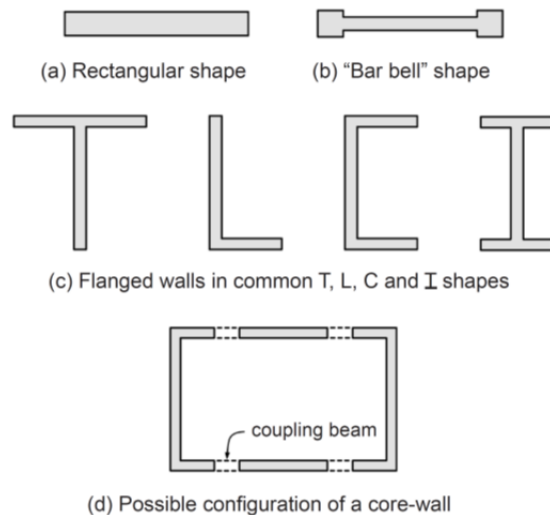


Figure 1: Typical wall configurations for US construction (NIST 2012)

Research results suggest the best earthquake performance is achieved when a symmetric configuration, in which lateral loading activates similarly sized and similarly reinforced compression and tension regions, is employed (Birely 2012). Examples of symmetric wall configurations include symmetrically reinforced rectangular (i.e. planar), barbell, H-shaped and I-shaped walls as well as coupled c-shaped walls, as shown in Figure 1.

In contrast to symmetric walls, asymmetric walls exhibit poorer seismic performance. From a simple moment-curvature assessment, this is apparent. Consider the T-shaped wall in Figure 1. When the flange is in tension, the base of the web is in compression. Clearly, the tension capacity of the flange greatly exceeds the compressive capacity. This results in the wall experiencing large compressive demands and, ultimately, the wall exhibits a relatively non-ductile compression-controlled failure.

This phenomenon and the potential for asymmetric walls to exhibit poor seismic performance have been demonstrated by research and damage observed following the 2010 Chilean earthquake. This is further demonstrated by empirical drift-capacity models, which were developed as part of this project (Birely et al. 2014) (Figure 2). Finally, a review of buildings exposed to the 2010 Chilean earthquake (NEHRP Consultants Joint Venture 2013) concluded that wall configuration contributed to localization and accumulation of damage; although for

Chilean buildings wall configurations were typically complex and damage was typically associated with floor-to-floor changes in wall configuration rather than asymmetry.

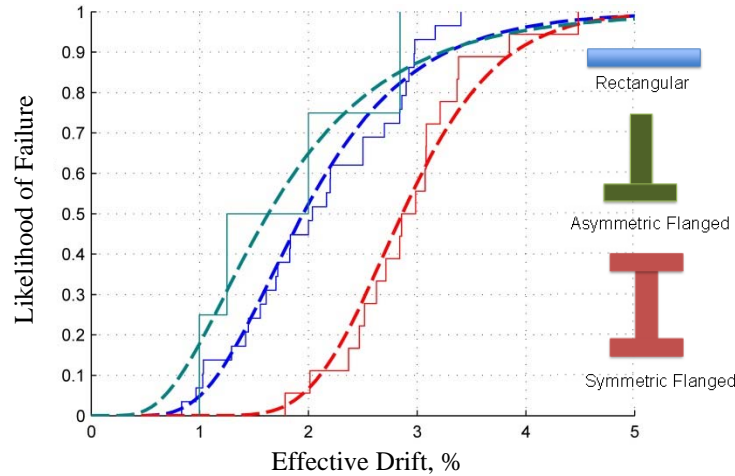


Figure 2: Probabilistic failure models for rectangular and asymmetric and symmetric flanged walls; failure is defined as loss of lateral load carrying capacity.

INITIAL SIZING

With wall configuration chosen to meet architectural constraints or provide enhanced seismic performance, it is recommended the wall be initially sized to mitigate large axial stress ratios and shear stress demands. These recommendations are supported by the prior research.

Figure 3 shows the drift capacity of wall specimens tested in the laboratory as a function of axial load ratio and shear stress ratio. In Figure 3, symbols indicate the failure mode of the wall: i) Flexural-Fracture (Flex.-Frac.), characterized by fracture of longitudinal reinforcement prior to or following buckling of the reinforcement (Figure 4), ii) Flexural-Compression (Flex.-Comp.), characterized by simultaneous crushing of confined boundary element concrete and buckling of longitudinal reinforcement (Figure 5), or iii) Shear, characterized by development of wide diagonal cracks within the web of the wall and/or crushing of web concrete (Table 1a).

An effective way to estimate the initial thickness of a concrete wall is to limit the axial stress ratio (ratio of applied load to gross-section compressive strength) resulting from gravity loading to 0.1. For walls that are part of a coupled wall system, earthquake loading activates coupling beams; coupling beam shear becomes axial tension or compression in the wall piers and significantly increases (or decreases) the wall axial load due to gravity alone. For walls in a coupled wall system, maximum axial compression load may be conservatively estimated as the axial load due to gravity loading plus the sum of the shear demands resulting from yielding of the majority of the coupling beams that frame into the wall. The data in Figure 3 show drift capacity versus axial load ratio for rectangular wall subjected to constant axial loading. These data suggest that drift capacity decreases with increasing axial load and that flexure-

compression failure is more likely to occur in walls with higher axial load ratios. Similar trends are observed for non-planar walls (Birely et al. 2014).

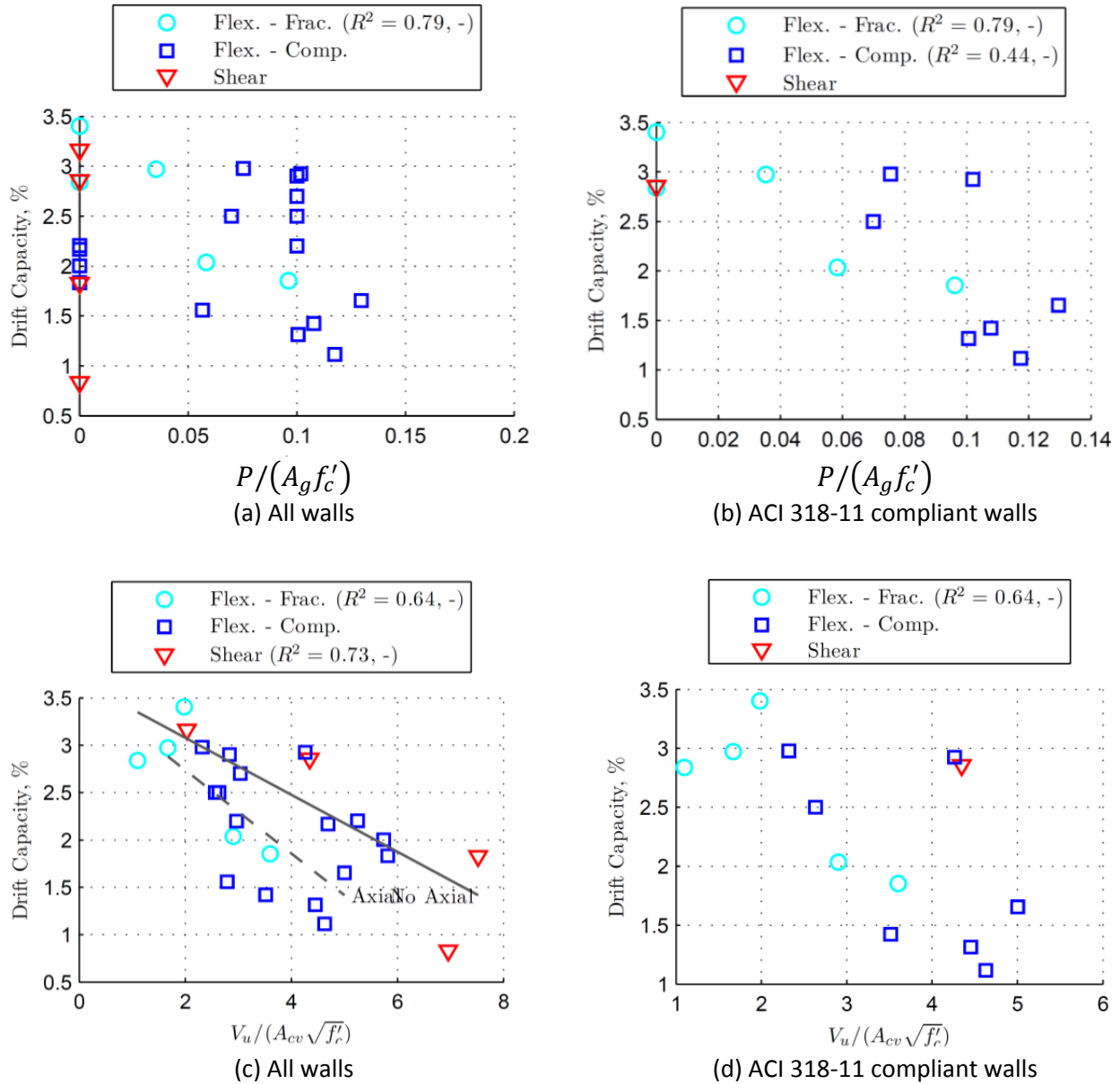


Figure 3: Drift capacity versus axial load ratio (a and b) and shear stress demand (c and d) for rectangular walls. Note that shear stress demand is normalized with respect to f'_c in psi.

In addition to initially sizing walls to meet the axial stress ratio limit, walls are also initially sized to limit the shear to a target shear stress demand under earthquake loading. Base shear demand may be estimated as

$$V_u = \frac{S_a W}{R_{NEW}} \quad (1)$$

where S_a is the ordinate of the earthquake design spectrum at the design period of the building, which may be estimated as $0.1N$ for a walled building where N is the number of stories, W is the seismic weight of the building, and R_{NEW} is a strength modification factor for walls developed as part of this study ($R_{NEW} = 2.5$ for planar or asymmetric walls and $R_{NEW} = 3.5$ for symmetric walls). The Tall Building Initiative Guidelines Working Group (2010) recommends initial sizing to achieve $V_u = 2\sqrt{f'_c}A_{cv}$ to $3\sqrt{f'_c}A_{cv}$ psi under service-level (50% probability of exceedance in 30 years) earthquake loading. Here it is recommended that walls be preliminarily sized to achieve these shear stress demands under design-level earthquake demands that do not include torsional effects; higher stresses values may be appropriate for preliminary sizing if the impact of torsion is considered. The ACI Code allows higher shear stress demands under factored design loads; however, these lower stress demands are recommended for initial sizing to account for increased shear demand due to dynamic amplification in walls exhibiting nonlinear flexural response under earthquake loading.

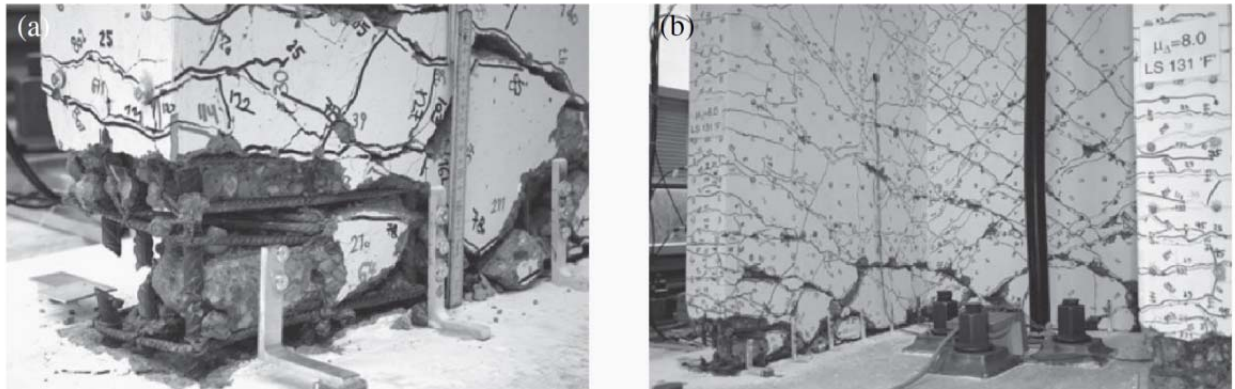


Figure 4: Flexural-tension failure of a U-shaped wall specimen subjected to bi-directional lateral loading and constant axial loading (Beyer et al. 2008). At the end of the test: (a) fractured longitudinal steel and (b) wall damage.



Figure 5: Flexural-compression failure of a T-shaped wall specimen subjected to bi-directional lateral loading and constant axial loading (Brueggen 2009). At the end of the test: (a) buckled longitudinal steel with crushed confined concrete removed and (b) wall damage.

ELASTIC ANALYSIS PROCEDURE

With walls sized initially for shear and axial demands, elastic modal response spectrum analysis (MRSA) is recommended to determine wall demands. The MRSA generates modal contributions to shear demand that are used in the proposed capacity-design procedure for shear that presented below. MRSA results are affected by model characteristics such as the components included in the structural model, the element formulations used to simulate the response of these components, the assumed stiffness of concrete components that exhibit cracking under service- and design-level loading, and the assumed viscous damping ratio. Here, two model parameters considered to be particularly important to demand assessment using MRSA are addressed: 1) the effective stiffness values that are used for flexure, shear and axial response of walls and coupling beams and 2) the viscous damping ratios that are used for primary response modes. Recommendations included here incorporate the results of recent research by Pugh (2012) addressing design of walled buildings and the modeling of hysteretic damping using viscous damping and elastic MRSA and by Turgeon (2011) and Mock et al. (2015) addressing the effective stiffness of coupling beams and planar and non-planar walls subjected to unidirectional and bidirectional lateral loading and recent research.

Effective Stiffnesses for Walls and Coupling Beams for Use in Elastic Analysis

When elastic analysis is used to determine component demands and story drifts under earthquake loading, it is necessary that reduced effective stiffnesses be used for concrete components to ensure accurate prediction of the i) building periods, and thus the earthquake demand experienced by the building, ii) the distribution of loads to individual components, and iii) the deformation experienced by individual components and thus the building system. In recent years, many research efforts have addressed the effective stiffness of concrete walls and coupling beams for use in elastic analysis to support seismic design, and many guidelines, standards and codes have been updated to reflect research results. Most of these existing recommendations were developed using data primarily from laboratory tests of planar walls subjected to unidirectional lateral loading, and Mock et al. (2015) conclude that bidirectional loading has minimal impact on the effective stiffness of nonplanar walls.

Research by Pugh (2015) addressed the design of walled buildings to achieve a flexure-controlled response mechanism and desired collapse risk under earthquake loading. Pugh employed elastic MRSA to determine design demands, with wall stiffness defined as presented in Table 1Table 2. Wall design progressed using the design procedure presented in this document, and nonlinear dynamic analysis was performed to verify that walled buildings exhibited acceptable performance. Thus, the effective stiffness values listed in Table 2 are recommended for use with the design process proposed in this document. Pugh (2015) did not consider coupled wall systems, and thus did not consider the effective stiffness of coupling beams. Mock et al. (2015) presents empirically derived effective stiffnesses for walls and coupling beams; these can be used to assess the relative stiffness of coupling beams and wall piers.

Table 2: Effective stiffness values used by Pugh (2015) for elastic MRSA of walled buildings to assess earthquake demands for design.

Component	Flexural Rigidity	Shear Rigidity	Axial Rigidity
Planar Wall	$0.5E_cI_g$	G_cA_{cv}	E_cA_g
Non-planar Wall	$0.5E_cI_g$	G_cA_{cv}	E_cA_g

Viscous Damping for MSRA

For linear elastic analysis, viscous damping is included to represent the energy dissipation resulting from nonlinear hysteretic response of structural components, which is not captured by the linear elastic model, as well as to represent inherent structural damping. Inherent structural damping is typically associated with the response of i) architectural cladding, partitions and finishes and ii) the foundation and soil. For linear analysis, a viscous damping ratio of 5% is typically assumed for all modes, and ASCE 7 (2010) design spectra are defined for 5% damping. However, Pugh (2012) demonstrates that for 6- to 30-story walls, the energy dissipation due to nonlinear flexural response of the walls is negligible. This suggest that the damping included in the linear elastic analysis represents inherent structural damping. Recent guidelines addressing nonlinear analysis for seismic design recommend viscous damping ratios for nonlinear analysis, which are intended to represent only inherent damping, ranging from 1% - 3% (Deierlein et al. 2010, TBI Working Group 2010, Willford et al. 2008). Thus, here it is recommended that a viscous damping ratio of 2% be used for primary modes for elastic MRSA of walled buildings. Use of 2% viscous damping requires modification of the ASCE 7 design spectrum per Naeim and Kircher (2001).

CALCULATION OF MOMENT DEMAND FOR WALL SECTION DESIGN

Per ASCE 7, base moment demand computed from MRSA is reduced using a response modification factor (R-factor); here response modification factors are proposed that depend on wall configuration and have been shown to provide acceptable risk of collapse for design and maximum-considered earthquake intensities. Moment demand up the height of the wall is determined using one of two previously proposed envelopes; these envelopes are shown to ensure that flexural yielding is isolated to locations identified by the engineer. Wall cross-sections are designed to meet strength requirements, with strength determined per the ACI Code.

ASCE 7 Response Modification Coefficients

ASCE 7 specifies that earthquake loads used for component design be equal to the loads determined from MRSA or the ASCE 7 equivalent lateral force (ELF) procedure, reduced by a response modification coefficient, $R_{ASCE} = 5$ for bearing walls and $R_{ASCE} = 6$ for building frame system walls. Use of response modification factors is expected to result in economical designs and walls that exhibit significant inelastic action under design-level earthquake loading. R-factor values for walls are predicated on walls maintaining strength through multiple inelastic response cycles to large inelastic deform demand levels.

FEMA P695 (2009) provides guidelines for determining R for new or existing systems to achieve the desired collapse risk. When considering R_{ASCE} for walls, it should be noted that ASCE 7-10 requires that 1) the fundamental first-mode building period used to determine seismic demands not exceed $C_u T_a$, where C_u is the specified upper limit on the calculated period, and T_a is the approximate fundamental period of the structure computed per ASCE 7, and 2) demands determined from MRSA cannot be taken less than 85% of those determined using the ELF procedure (note that it is expected that ASCE 7-16 will require MRSA loads be scaled to 100% of ELF loads). Since MRSA analysis of slender walls typically results in 1) a fundamental building period that is larger than the ASCE 7 design period for walls and 2) base shear and moment demands that are less than those determined from the ELF procedure, the *effective* R -factors for MRSA-based designs are significantly less than those specified in ASCE 7. Pugh concludes that $R_{ASCE} = 5,6$ results in effective R factors for MRSA-based designs of $R_{eff} = 3,4$.

Recent research by Pugh (2012) demonstrates that for walls exhibiting a flexural response mechanism, use of ASCE 7-10 to determine earthquake demands, including $R_{ASCE} = 5$ or 6 , results in walls that have an unacceptably high probability of failure under earthquake loading. Pugh shows also that to achieve the same failure risk for all wall configurations, smaller R factors are required for planar walls than for symmetric flanged walls. This is attributed to the larger drift capacity of symmetric flanged walls (Birely et al. 2014) that results from symmetric flanged walls experiencing relatively smaller compressive demands distributed over relatively larger flange areas.

On the basis of the Pugh work and given that asymmetric non-planar walls (i.e. T-shaped, L-shaped and C-shaped walls subjected to loading parallel to the flanges) exhibit drift capacities that are comparable to planar walls (Birely et al. 2014) and that like planar walls, asymmetric non-planar walls could be expected to exhibit relatively higher compressive demands that are distributed over relatively small wall areas, it is recommended that

1. The moment demand at the critical section of the wall is computed using MRSA and the modeling recommendations presented above.
2. Design of planar and asymmetric non-planar walls use $R_{NEW} = 2.5$ and design of non-planar symmetric walls and core-wall systems use $R_{NEW} = 3.5$. Here it should be noted that these response modification factors are applied directly to the demands determined from MRSA, not to MRSA demands which have been scaled to match the base shear demand determined using the ELF procedure, as is currently required in ASCE 7. The $R_{NEW} = 2.5$ and 3.5 applied to the *unscaled* MRSA demands are, on average, approximately equivalent to the current ASCE $R_{ASCE} = 5$ for bearing walls that is applied to *scaled* MRSA demands.

Moment Envelope for Flexural Design

In regions where nonlinear flexural response is expected, relatively large volumes of closely spaced transverse reinforcement are required to confine concrete, delay buckling of longitudinal reinforcement and, thereby, enable the wall to maintain flexural strength through multiple nonlinear load cycles to large inelastic deformation demands. Thus, it is desirable that

nonlinear flexural response be confined to expected locations so that large volumes of transverse reinforcement are required only in these regions. Previous research has resulted in a number of approaches for defining the moment demand envelope, up the height of the wall, to ensure that flexural yielding occurs only in expected locations.

Pugh (2012) used the results of incremental time-history analysis (ITHA) of buildings ranging in height from 6 to 24 stories to investigate previously proposed and currently employed approaches for defining the moment demand envelope, including i) demand determined by MRSA, ii) the envelope recommended by Paulay and Priestley (1992) and SEAOC (2006), in which maximum moment at the base of the wall is extended up to a height equal to the in-plane length of the wall and then moment demand diminishes linearly to zero at the top of the wall, and iii) the dual-hinge approach recommended by Panagiotou and Restrepo (2009) in which wall demands are assumed to be defined by MRSA and capacities are established such that yielding occurs at the base of wall and at a second-hinge location above mid-height of the wall. Figure 6 shows moment demand up the height of a 12-story wall as determined using these three approaches and the factored moment capacity designed to meet these demands. Figure 7 shows the median simulated curvature ductility demand for 12-story walls designed using the three moment envelopes and subjected to a suite of synthetic motions scaled to the MCE spectrum. Data such as that shown in Figure 7 indicate that only the Paulay and Priestley (1992) and Panagiotou and Restrepo (2009) methods resulted in significant inelastic action being limited to expected locations. Thus, these methods are recommended for use in design.

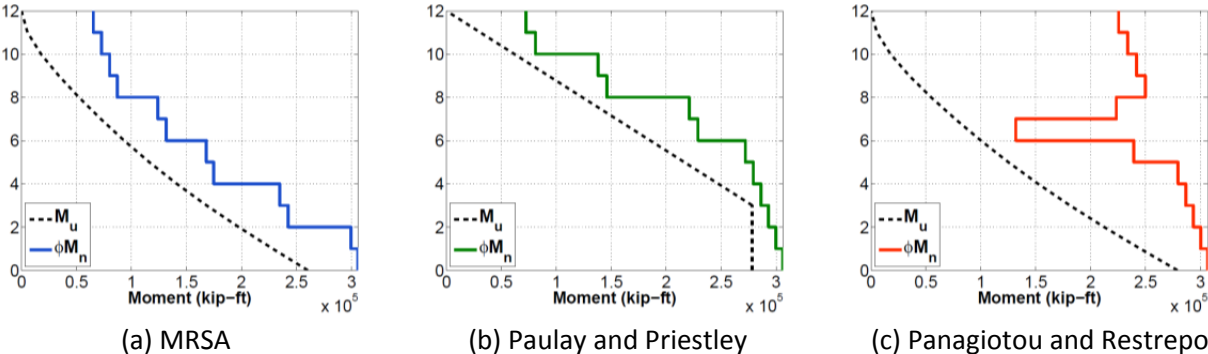


Figure 6: Moment demand envelope used for design, M_u , and factored moment capacity, ϕM_n . Note that the vertical axis is story height. Note also that small changes in factored moment capacity, ϕM_n , occur at each story due to changes in the gravity load and not to changes in section design; large changes in moment capacity indicate a change in section design.

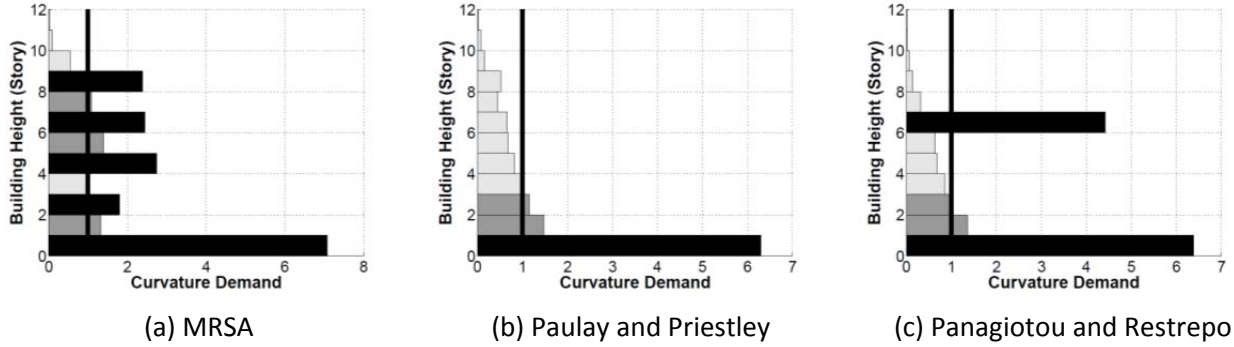


Figure 7: Median curvature ductility demand, ϕ/ϕ_{yield} , for three flexural demand envelopes for a 12-story walled building subjected to a suite of seven synthetic motions scaled to the MCE.

CALCULATION OF SHEAR DEMAND FOR WALL DESIGN

Many design codes (e.g. CSA A23.3, NZ 3101) require and guidelines (e.g. SEAOC 2008) and researchers (e.g. Eibl and Keintzel 1988, Priestley et al. 2007, Rejec et al., 2012, Pugh 2012) recommend capacity-design procedures for shear design of walls. Using these procedures, shear demands determined from analysis (V_u) are amplified for design (V'_u) as follows:

$$V'_u = \omega_v \Omega_{flex} V_u \quad (2)$$

where V_u is the reduced shear demand computed using the results of MRSA and the response modification factors recommended above ($R_{NEW} = 2.5$ for symmetric flanged walls and $R_{NEW} = 3.5$ for other configurations), and Ω_{flex} and ω_v are intended to account for increased shear demand resulting from flexural over-strength and dynamic amplification, respectively.

Under earthquake loading, slender walls are expected to exhibit a flexural response mechanism, with flexural yielding typically isolated to a critical section at or near the base of the wall. Thus, maximum shear demand is determined by the flexural strength of the wall. The over-strength factor in Eq. 1, Ω_{flex} , is intended to account for the additional shear demand associated with walls achieving an actual flexural strength that exceeds the demand used for flexural design. Typically, the moment at the critical section of the wall is dominated by the contribution from the first dynamic response mode. Thus, flexural yielding at the critical section could be expected to limit shear demand due to first-mode response but not necessarily to limit shear demand due to higher mode response. The dynamic amplification factor in Eq. 1, ω_v , is intended to account for the additional shear demand associated with essentially elastic higher-mode response.

To develop recommendations for capacity-design for shear, Pugh (2012) designed a series of walled buildings ranging in height from 6- to 30-stories; buildings were designed for seismic design category D using the ASCE 7-10 design spectrum, MRSA with an elastic model and the effective stiffness values listed in Table 2, and the ACI Code. The response of these buildings to earthquake loading was assessed using nonlinear ITHA and a suite of synthetic ground motions developed to match the ASCE 7 design spectrum. Synthetic motions were employed to reduce

the difference between demands determined from a design spectrum, which were used for design, and demands resulting from earthquake acceleration histories, which were used for assessment. Pugh (2012) provides details of the analyses. Pugh found that for these buildings, the ratio of actual flexural strength to flexural demand at the critical section of the wall was approximately 1.4. Thus, Pugh recommends $\Omega_{flex} = 1.4$ in Eq. 1; this is consistent with NEHRP (2011) and Priestley et al. (2007).

Pugh (2012) also evaluated previously proposed recommendations (Eibl et al. 1988, SEAOC 2006, Priestley et al. 2007, NZS 3101 2008) for defining ω_v in Eq. 1. Pugh found that the method developed by Eibl et al. (1988) provided the best prediction of shear demand, but that this method significantly overestimates dynamic amplification for longer period buildings (first mode period greater than approximately 2.0 seconds) for which the second or third dynamic response mode, rather than the first, dominates response. Eibl et al. proposed that dynamic amplification be addressed by using MRSA to determine demands, reducing the first mode contribution to shear using the R-factor used for computing moment demand, and using elastic (i.e. unreduced) higher mode contributions to shear. Pugh found that the conservatism of this method for longer period structures could be mitigated by modifying the method such that shear demand is determined using MRSA with the mode that contributes most to shear demand reduced using the R-factor used for moment demand and using elastic, unreduced contributions for all other modes.

Thus, it is recommended that shear design be accomplished as follows:

$$\phi V_n \geq \gamma V_u' \quad (3)$$

where ϕ is 0.75 as recommended by ACI 318 for shear demand computed using a capacity-design approach, V_n is the shear strength of the wall computed per ACI 318, $\gamma = 1.1$ to achieve a desirable likelihood of shear capacity exceeding demand, and V_u' is the shear demand computed using an elastic model and MRSA with modal contributions to shear reduced and combined as follows:

$$V_u' = \sqrt{\left(\frac{\Omega_{flex} V_1}{R_{NEW}}\right)^2 + V_2^2 + V_3^2 + \dots V_n} \text{ for } V_1 > V_2 > V_3 > \dots > V_n \quad (4a)$$

$$V_u' = \sqrt{V_1^2 + \left(\frac{\Omega_{flex} V_2}{R_{NEW}}\right)^2 + V_3^2 + \dots V_n} \text{ for } V_2 > V_1 > V_3 > \dots > V_n \quad (4b)$$

where V_i is the i^{th} mode contribution to the shear demand, R_{NEW} is the strength reduction factor of 2.5 or 3.5, as is appropriate based on wall configuration, and $\Omega_{flex} = 1.4$ to account for flexural overstrength. The above employs the SRSS rule to combine modal contributions to the shear; alternatively the CQC method may be used.

Pugh designed a series of 6- to 30-story buildings using the above approach and subjected these walls to ITHA. For these walls, the ratio of maximum shear demand under design-level earthquake loading to *factored* shear strength was less than 1.0 and that ratio of maximum

shear demand under maximum considered earthquake loading to *actual* shear strength was also less than 1.0.

SUMMARY OF DESIGN RECOMMENDATIONS FOR WALLS

The above recommendations for seismic design of concrete walls are summarized by the following design process:

1. Configure walls to have a planar, asymmetric flanged, or symmetric flanged geometry.
2. Size walls to achieve a base shear demand of $V_u = 6\sqrt{f'_c}A_{cv}$ for shear demand estimated using Eq. 1 and an axial demand due to gravity loads of less than $0.1f'_cA_g$, if torsional demands are included.
3. Complete a MRSA of the building using a 2% damped design spectrum to define earthquake loads and wall effective stiffnesses of $0.5E_cI_g$, G_cA_g , and E_cA_g .
4. Determine the moment demand envelope to be used for design using the moment demand at the critical section from MRSA, an $R_{NEW} = 2.5$ for planar and asymmetric nonplanar walls or $R_{NEW} = 3.5$ for symmetric nonplanar walls to reduce demands, and either the envelope recommended by Paulay and Priestley (1992) or that recommended by Panagiotou and Restrepo (2009). Here it should be noted that the R_{NEW} response modification factors are applied directly to the demands determined from MRSA, not to MRSA demands which have been scaled to match the base shear demand determined using the ELF procedure, as is currently required in ASCE 7. The $R_{NEW} = 2.5$ and 3.5 applied to the *unscaled* MRSA demands are, on average, approximately equivalent to the current ASCE $R_{ASCE} = 5$ for bearing walls that is applied to *scaled* MRSA demands.
5. Determine the shear demand envelope to be used for design using MRSA results. To account for dynamic amplification, shear demand is computed as the SRSS or CQC combination of the shear for the response mode that contributes most to total shear demand, reduced using the R-factor used for flexural design and amplified by $\Omega_{flex} = 1.4$ to account for flexural over-strength, and the elastic, unreduced shears for all other modes.

NONLINEAR ANALYSIS FOR PERFORMANCE ASSESSMENT

Nonlinear analysis is beneficial for assessment of the earthquake performance of walled buildings. A wide range of models have been used to simulate the nonlinear behavior of concrete walls. Pugh (2012) reviewed nonlinear response models used currently in research and practice and found that fiber-type beam-column elements provided the greatest potential for accurate, objective, numerically efficient and robust simulation of the nonlinear response of concrete walls. Pugh et al. (2015) presents recommendations for using fiber-type force-based beam-column elements for simulating wall response and demonstrates that using these recommendations wall response, including lateral strength loss, can be accurately simulated. The modeling approach developed by Pugh et al. is validated for planar walls with a range of design parameters and for c-shaped wall subjected to uni-directional and bi-directional loading. The modeling approach developed by Pugh et al. is recommended for assessing wall performance.

Defining characteristics of the modeling approach presented in detail in Pugh et al. (2015) are as follows.

- Individual wall piers are modeled using force-based fiber-type beam-column elements. The force-based beam-column element is a two-node element that employs the assumptions of a linear moment distribution and constant shear and axial load distributions along the length of the element. Within the element, flexural response is decoupled from shear response. A fiber-type section model is used to simulate nonlinear flexural response of the wall section, with the assumption of a linear strain distribution across the section. A linear or nonlinear shear response model may be employed at the section level.
- Given the assumptions of a linear moment distribution and constant shear and axial load distributions along the length of the element, one element is required per story. To provide accurate simulation of wall response, five fiber sections are required along the length of each element if a Gauss-Lobatto numerical integration scheme is used. Also to provide accurate simulation of response under cyclic loading, a fiber thickness that results in approximately 30 fibers within the boundary element region of the wall section is recommended.
- For most slender wall designs, loss of lateral load carrying capacity is due to flexural failure and is characterized by gradual softening at the section level. Gradual softening results in localization of nonlinear deformations at a single softening section and requires regularization of material response to achieve accurate and mesh-objective simulation of drift capacity. To regularize material response, the post-peak (concrete) or post-yield (reinforcing steel) portion of the stress-strain curve is defined using a measure of dissipated energy and the integration length associated with the fiber section. Pugh et al. (2015) provide crushing energies for unconfined and confined concrete in walls and a procedure for defining the post-yield dissipated energy for reinforcing steel. Note that this implies that multiple unconfined and confined concrete and reinforcing steel stress-strain response curves are required for definition of a single force-based fiber-type beam-column element.

PERFORMANCE ASSESSMENT

Assessment of concrete wall performance under earthquake loading is best accomplished using the results of nonlinear analysis that employ regularized material models to enable accurate predictions of the onset of strength loss. The following sections provide guidance on using nonlinear analysis results to assess wall performance.

Performance assessment using computed strain demands

Inclusion of material regularization enables accurate simulation of response, including drift capacity. However, regularization of material response results in modification of the post-peak stress strain response for concrete and steel such that computed strain demands cannot be used directly to assess the performance state of the material and component. To enable assessment of component performance using simulated material strains, three damage ratios

are recommended. These are the spalling damage ratio (SDR), the crushing damage ratio (CDR), and tension damage (rupture) ratio (TDR), which are defined as follows:

$$SDR = \frac{\varepsilon_c}{\varepsilon_{85c}} \quad (5)$$

$$CDR = \frac{\varepsilon_c}{\varepsilon_{20c}} \quad (6)$$

$$TDR = \frac{\varepsilon_s}{\varepsilon'_u} \quad (7)$$

where ε_c is the maximum simulated concrete compressive strain, ε_{85c} is the (regularized) concrete compressive strain at which 15% compressive strength loss is predicted to occur, ε_{20c} is the (regularized) concrete compressive strain at which 80% compressive strength loss is predicted to occur, ε_s is the maximum simulated longitudinal reinforcement tensile strain, and ε'_u is (regularized) tensile strain at which rupture of longitudinal reinforcement is predicted to occur. An SDR greater than 1.0 indicates that significant cracking and spalling of cover concrete could be expected and that minor repair of the structure would likely be required. A CDR or TDR greater than 1.0 indicates failure and that the wall would likely require replacement.

Performance assessment using fragility functions

The performance of concrete walls may be assessed also using empirical damage-prediction models. These models typically define the likelihood of a region of the wall meeting or exceeding a given damage state as a function of the maximum story drift or local rotation demand experienced by that region of the wall. These models are typically referred to as fragility functions. To facilitate application in practice, fragility functions are typically defined using the lognormal cumulative probability function. Fragility functions defining structural component damage as a function of maximum story drift and other earthquake demand measures are included in FEMA P-58 Performance Assessment of Buildings (FEMA 2012).

As part of the current project, data from 88 experimental tests were used to develop fragility functions defining the likelihood of walls meeting or exceeding five damage states ranging from cosmetic damage to failure requiring replacement of the wall. Specimens used to develop the fragility functions had various configurations (rectangular, barbell and C-, T-, L-, H- and I-shaped), were slender with a shear span ratio $\left(\frac{M_{base}}{V_{base}L_w}\right)$ greater than 2.0, and were subjected quasi-static unidirectional and bidirectional lateral load histories. The damage states considered included the following:

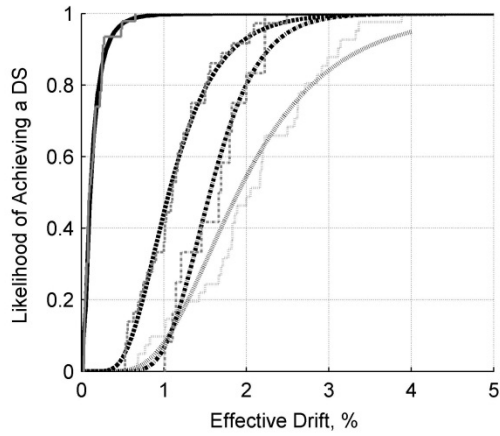
- DS1: Initial cracking and/or initial yielding of reinforcing steel requiring only cosmetic repair.
- DS2: Initial spalling of cover concrete; epoxy injection of cracks and patching of spalled concrete is required to restore the wall to essentially pre-earthquake condition.
- DS3: Spalling of cover concrete that exposes longitudinal reinforcement; removal and replacement of concrete surrounding longitudinal reinforcement is required to restore the wall to essentially pre-earthquake condition.

DS4: Crushing of core confined concrete, crushing of unconfined web concrete, buckling of longitudinal reinforcement, fracture of longitudinal or horizontal reinforcement, or shear failure; the damaged portion or the entire wall must be replaced to restore the system to pre-earthquake condition.

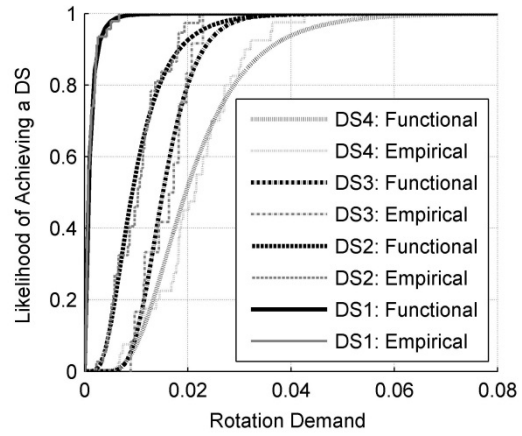
The impact on damage progression of various design and load parameters was assessed. Parameters considered included wall configuration (rectangular, barbell, non-planar), axial load ratio ($\lambda_N < 0.1$ and $\lambda_N \geq 0.1$, where $\lambda_N = P/f'_c A_g$), unidirectional versus bidirectional lateral loading, shear span ratio, maximum shear stress demand, ratio of maximum shear demand to shear capacity per the ACI Code. It was found that

1. Walls with lower axial load ratios ($\lambda_N < 0.1$) exhibited larger drift capacities (i.e. DS4 is reached at larger drifts).
2. For the more severe damage states (DS3 – DS4), the onset of the damage state occurred at a lower drift for rectangular walls than for barbell or nonplanar walls. Note that one exception to this was for DS3 for which the onset of damage in barbell walls occurred at a lower drift than for rectangular and non-planar walls.
3. For non-planar walls, application of unidirectional versus bidirectional lateral loading had no impact on damage progression.
4. Shear span ratio and shear demand had no impact on damage progression.

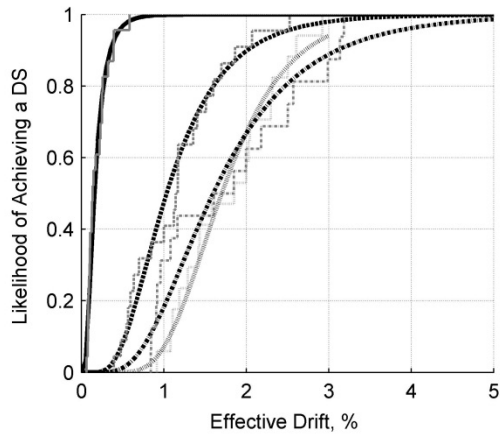
Figure 8 - Figure 10 show fragility functions for DS1 – DS4 for walls with low and high axial load ratios (Figure 8), as a function of wall configuration (Figure 9), and as a function of lateral load history (Figure 10). In these fragility functions earthquake demand is defined by maximum specimen drift at the height of the effective shear load (i.e. at a height of M_{base}/V_{base}) and by maximum rotation demand for a plastic hinge of length $0.5L_w$. Both the empirical CDF and lognormal CDF fit to the empirical data are provided. Table 3 - Table 5 provide data associated with the CDFs in Figure 8 - Figure 10; data include the number of test specimens for which data were available for use in calibrating the CDFs, the median drift (θ) and coefficient of variation (β) defining the lognormal CDFs, and if the lognormal CDF passes the Lilliefors goodness-of-fit test for the given data set.



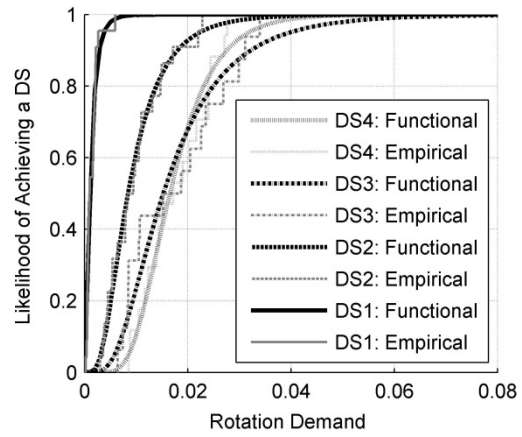
(a) Effective drift, $\lambda_N < 0.10$



(b) Rotation demand, $\lambda_N < 0.10$

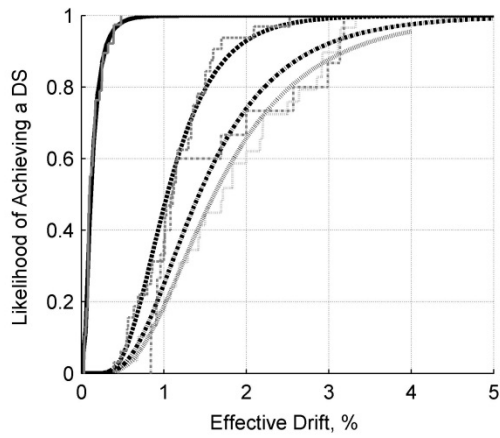


(c) Effective drift, $\lambda_N \geq 0.10$

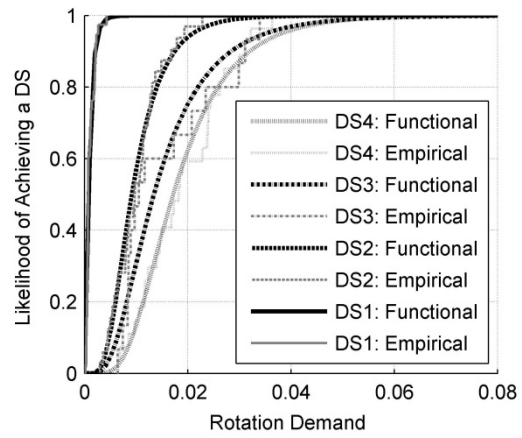


(d) Rotation demand, $\lambda_N \geq 0.10$

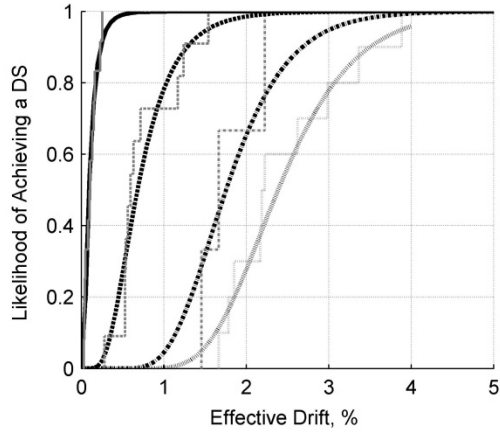
Figure 8: Fragility functions for slender reinforced concrete walls based on axial load ratio.



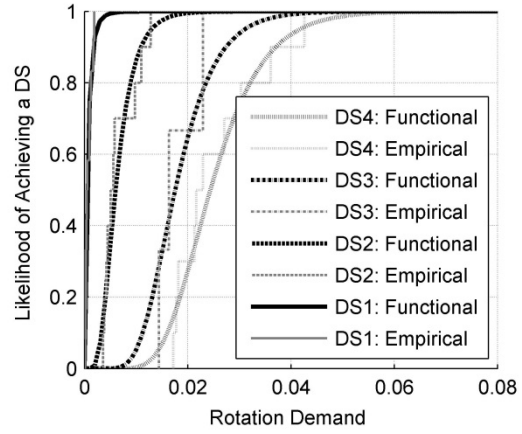
(a) Effective drift, rectangular walls



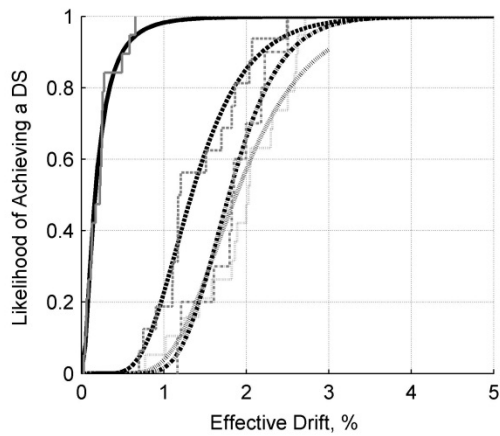
(b) Rotation demand, rectangular walls



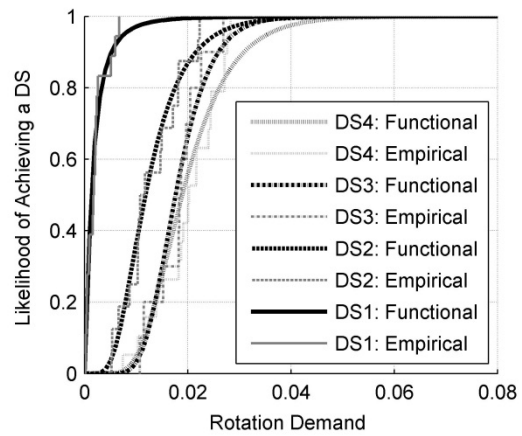
(c) Effective drift, barbell walls



(d) Rotation demand, barbell walls



(e) Effective drift, flanged walls



(f) Rotation demand, flanged walls

Figure 9: Fragility functions for slender reinforced concrete walls based on wall configuration.

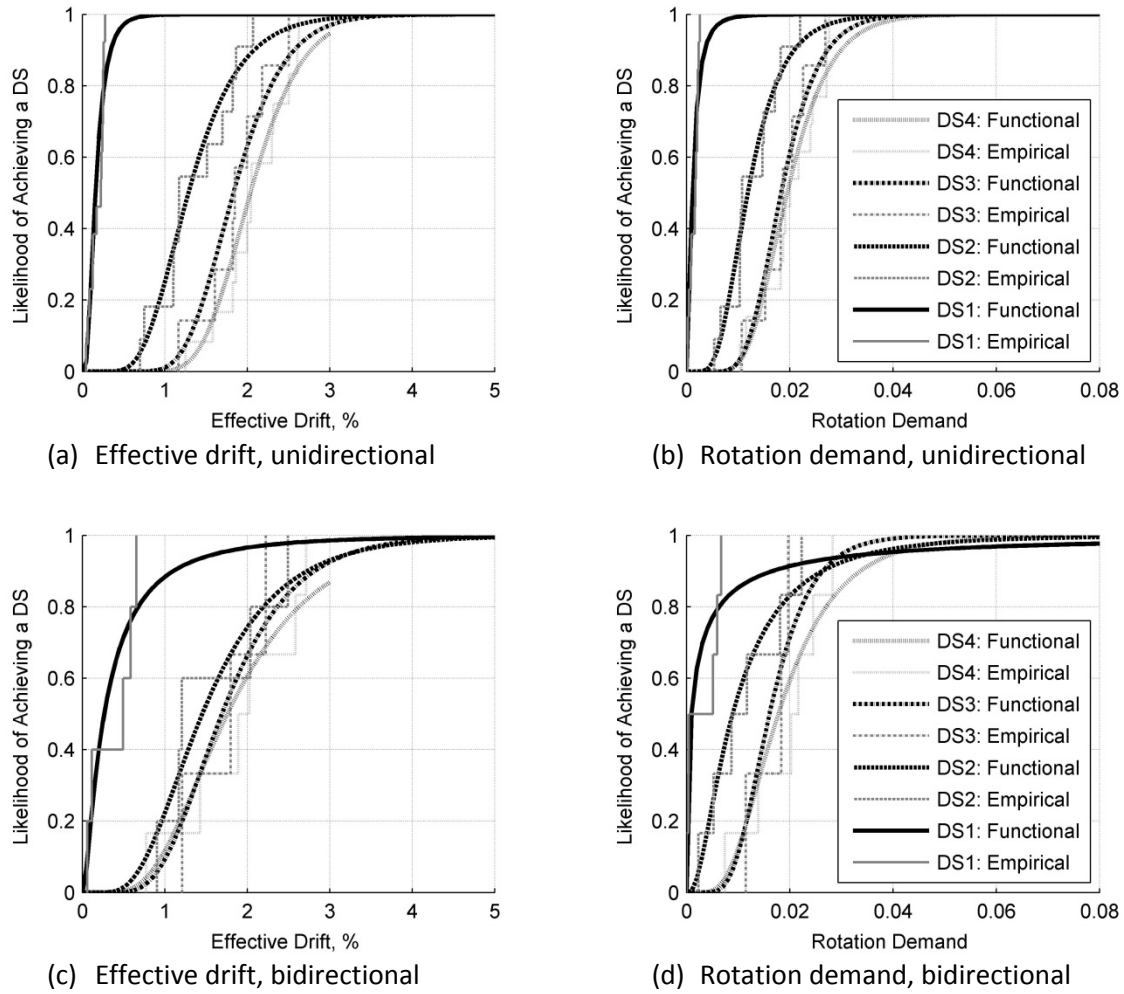


Figure 10: Fragility functions for flanged slender reinforced concrete walls based type of loading (unidirectional versus bidirectional).

Table 3: Fragility function parameters and evaluation of goodness-of-fit for all walls as a function of axial load.

		$\lambda_N < 0.10$				$\lambda_N \geq 0.10$			
		# Tests	θ	β_d	Correct CDF	# Tests	θ	β_d	Correct CDF
Effective Drift	DS1	47	0.11	0.79	T	23	0.16	0.61	T
	DS2	36	1.07	0.41	T	22	1.03	0.51	T
	DS3	12	1.56	0.28	T	16	1.6	0.51	T
	DS4	40	1.9	0.45	F	17	1.7	0.35	T
Hinge Rotation	DS1	46	0.8×10^{-3}	0.91	T	23	1.1×10^{-3}	0.73	T
	DS2	37	9.3×10^{-3}	0.53	T	22	8.5×10^{-3}	0.58	T
	DS3	12	15.2×10^{-3}	0.31	T	16	15.3×10^{-3}	0.57	T
	DS4	40	19.6×10^{-3}	0.45	F	17	16.5×10^{-3}	0.39	T

Table 4: Fragility function parameters and evaluation of goodness-of-fit for barbell and flanged walls.

		Rectangular				Barbell				Flanged			
		# Tests	θ	β_d	Correct CDF	# Tests	θ	β_d	Correct CDF	# Tests	θ	β_d	Correct CDF
Effective Drift	DS1	66	0.12	0.69	T	12	0.09	0.71	T	19	0.17	0.84	T
	DS2	48	1.04	0.43	T	11	0.68	0.48	T	16	1.34	0.37	T
	DS3	14	1.43	0.52	F	3	1.76	0.22	-	10	1.79	0.25	T
	DS4	60	1.61	0.53	T	10	2.40	0.28	T	19	1.88	0.34	F
Hinge Rotation	DS1	66	0.9×10^{-3}	0.68	F	12	0.6×10^{-3}	0.86	T	18	1.4×10^{-3}	1.05	T
	DS2	48	9.2×10^{-3}	0.49	T	10	6.0×10^{-3}	0.46	T	16	11.8×10^{-3}	0.46	T
	DS3	14	13.4×10^{-3}	0.58	T	3	17×10^{-3}	0.24	-	10	17.6×10^{-3}	0.29	T
	DS4	60	17.2×10^{-3}	0.48	T	10	24.4×10^{-3}	0.31	T	19	18.9×10^{-3}	0.37	T

Table 5: Fragility function parameters and evaluation of goodness-of-fit for uni- and bi-directionally loaded flanged walls.

		Uni-directional				Bi-directional			
		# Tests	θ	β_d	Correct CDF	# Tests	θ	β_d	Correct CDF
Effective Drift	DS1	13	0.16	0.59	F	5	0.27	1.08	T
	DS2	11	1.29	0.36	T	5	1.45	0.42	T
	DS3	7	1.83	0.24	T	3	1.69	0.31	-
	DS4	12	2.04	0.22	T	6	1.76	0.47	T
Hinge Rotation	DS1	13	1.2×10^{-3}	0.86	F	6	1.0×10^{-3}	2.21	T
	DS2	11	11.9×10^{-3}	0.43	T	6	8.9×10^{-3}	0.84	T
	DS3	7	18.3×10^{-3}	0.30	T	3	16.1×10^{-3}	0.29	-
	DS4	13	19.5×10^{-3}	0.32	T	6	17.8×10^{-3}	0.49	T

ACKNOWLEDGEMENTS

The research presented herein was funded by the Charles Pankow Foundation and the National Science Foundation through the Network for Earthquake Engineering Simulation Research Program, Grant CMS-042157, Joy Pauschke, program manager. Any opinions, findings, and conclusions or recommendations expressed in this material are those of the authors and do not necessarily reflect the views of the Charles Pankow Foundation or the National Science Foundation.

REFERENCES

1. Applied Technology Council (ATC). *PEER/ATC 72-1, Modeling and Acceptance Criteria for Seismic Design and Analysis of Tall Buildings*. A report prepared for the Pacific Earthquake Engineering Research Institute by the Applied Technology Council, 2010, 242 pp.

2. American Concrete Institute Committee 318. *Building Code Requirements for Structural Concrete (ACI 318-11) and Commentary (ACI 318-11)*. American Concrete Institute, Farmington Hills, MI, 2011.
3. ASCE. *Minimum Design Loads for Buildings and Other Structures, ASCE/SEI 7-10*. American Society of Civil Engineers, Reston, Virginia, 2007.
4. Birely AC. "Seismic performance of slender reinforced concrete structural walls." *PhD Dissertation*, University of Washington, 2012, 983 pp.
5. Blakeley R, Cooney R, Megget L. "Seismic shear loading at flexural capacity in cantilever wall structures." *Bulletin of the New Zealand Society for Earthquake Engineering* 1975; 8(4): 278–290.
6. Canadian Standards Association (CSA). *CSA A23.3 Design of concrete structures*, 2010.
7. Chiaramonte MM. "An analysis of conventional and improved marginal wharves." *MS Thesis*. University of Washington, Seattle 2011.
8. Coleman J, Spacone E. "Localization issues in force-based frame elements." *Journal of Structural Engineering, ASCE* 2001; 127(11): 1257-1265.
9. Deierlein G, Reinhorn A, Willford M (2010). *Nonlinear Structural Analysis for Seismic Design: A Guide for Practicing Engineers*, NEHRP Seismic Design Technical Brief No. 4, NIST GCR 10-917-5, National Institute of Standards and Technology, Gaithersburg, MD.
10. Eibl KE. "Seismic design shear forces in RC cantilever shear wall structures." *European Earthquake Engineering* 1990; 3: 7–16.
11. Federal Emergency Management Agency (FEMA). *Seismic Performance Assessment of Buildings, FEMA P-58-1,2,3 Report*. Prepared by the Applied Technology Council for FEMA, Washington, DC, 2012.
12. Federal Emergency Management Agency (FEMA). *Quantification of building seismic performance factors, FEMA P-695 Report*. Prepared by the Applied Technology Council for FEMA, Washington, DC, 2009.
13. Ghosh S. *Required shear strength of earthquake-resistant reinforced concrete shear walls*. Fajfar P, Krawinkler H, Eds. London, UK: Elsevier, 1992.
14. ICC. *International Building Code*, I. C. Conference, Ed. Country Club Hills, IL: IBC, 2006.
15. Krawinkler H. "Importance of good nonlinear analysis." *The Structural Design of Tall and Special Buildings* 2006; 15(5): 515–531.
16. Lowes LN, Lehman DE, Birely AC, Kuchma DA, Marly K, Hart CR. "Earthquake response of slender planar concrete walls with modern detailing" *Engineering Structures* 2012; 43: 31-47.
17. Lowes LN, Oyen P, Lehman DE. "Evaluation and Calibration of Load-Deformation Models for Concrete Walls." *ACI-SP 265: Thomas T.C. Hsu Symposium: Shear and Torsion in Concrete Structures*. Ed. Belarbi A, Mo YL, Ayoub A. Farmington Hills: American Concrete Institute, 2009: 171-198.

18. Lehman DE, Turgeon, J, Birely AC, Hart CR, Marley KP, Kuchma DA, Lowes LN. "Seismic behavior of a modern concrete coupled wall." *Journal of Structural Engineering, ASCE* 2013; 139: 1371-1381.
19. Mock A, Behrouzi A, Lowes LN, Lehman DE, Kuchma DA (2015). "Empirically Derived Effective Stress Expressions for Elastic Analysis of Concrete Walls." Final Report to the Charles Pankow Foundation. 14 pp.
20. Mohr D. "Nonlinear analysis and performance based design methods for reinforced concrete coupled shear walls." *MS thesis*, Dept. of Civil and Environmental Engineering, University of Washington, Seattle, WA, 2007.
21. Naeim F, Kircher C. "On the damping adjustment factor for earthquake response spectra." *Journal of Structural Engineering, ASCE* 2001; 81(6): 1590–1607.
22. National Institute of Standards and Testing (NIST). *Seismic Design of Cast-in-Place Concrete Special Structural Walls and Coupling Beams: A Guide for Practicing Engineers, NIST GCR 11-917-11, NEHRP Seismic Design Technical Brief No. 6*. Prepared by the NEHRP Consultants Joint Venture for NIST, Gaithersburg, Maryland. 2011.
23. NEHRP Consultants Joint Venture. *Final report on Task Order 21: Analysis of Seismic Performance of RC Buildings in the 2010 Chile Earthquake, Including Effects of Non-Seismic-Force-Resisting Building Structural Elements*. 2013.
24. New Zealand Standards (NZS). *Concrete Structures Standard, Part 1: The Design of Concrete Structures: Part 2: Commentary on the Design of Concrete Structures*, S. N. Zealand, Ed. Wellington, New Zealand: NZS 3103, 2006.
25. Panagiotou M, Restrepo J. "Dual-plastic hinge design concept for reducing higher-mode effects on high-rise cantilever wall buildings." *Earthquake Engineering & Structural Dynamics* 2009; 38(12).
26. Paulay T, Priestley N. *Seismic Design of Reinforced Concrete and Masonry Buildings*. Interscience, 1992.
27. Priestley N, Calvi G, Kowalsky M. *Displacement-Based Seismic Design of Structures*. 2007.
28. Pugh JS. "Numerical simulation of walls and seismic design recommendations for walled buildings." *PhD Dissertation*, University of Washington, 2012, 448 pp.
29. Pugh JS, Lowes LN, Lehman DE (2015). "Nonlinear line-element modeling of flexural reinforced concrete walls" *Engineering Structures* (104): 174-192.
30. Rejec K, Isakovic T, Fischinger M. "Seismic Shear Force Magnification in RC Cantilever Structural Walls, Designed According to Eurocode 8." *Bulletin of Earthquake Engineering* 2012; 10(2): 567-586.
31. Structural Engineers Association of California. *IBC Structural/Seismic Design Manual Volume 3: Building Design Examples for Steel and Concrete*, ICC, Ed. Sacramento, CA: ICC, 2006.

32. Thomsen J, Wallace J. "Displacement-based design of slender reinforced concrete structural walls – experimental verification." *Journal of Structural Engineering, ASCE* 2004; 130(4): 618–630.
33. Tall Building Initiative Guidelines Working Group. Guidelines for Performance-Based Seismic Design of Tall Buildings. *PEER Report 2010/05*. Berkeley, California: Pacific Earthquake Engineering Research Center, University of California, 2010.
34. Willford M, Whittaker A, Klemencic R. (2008). *Recommendations for the seismic design of high-rise buildings*, Council on Tall Buildings and Urban Habitat, Illinois Institute of Technology, Chicago, IL.
35. Wong PS, Vecchio FJ. *VecTor2 and FormWorks User's Manual*. University of Toronto, 2006.
36. Yassin M. "Nonlinear analysis of prestressed concrete structures under monotonic and cyclic loads." *Ph.D. Dissertation*, Dept. of Civil and Environmental Engineering, University of California, Berkeley, Berkeley, CA, 1994.